

Cite this: *Chem. Sci.*, 2023, 14, 14271

All publication charges for this article have been paid for by the Royal Society of Chemistry

O–H bond activation of β,γ -unsaturated oximes via hydrogen atom transfer (HAT) and photoredox dual catalysis†

Liang Yi,^{ab} Chen Zhu,^{id a} Xiangyu Chen,^{id b} Huifeng Yue,^a Tengfei Ji,^b Yiqiao Ma,^{id b} Yuanyuan Cao,^b Rajesh Kancharla^{id a} and Magnus Rueping^{id *a}

Hydrogen atom transfer (HAT) and photoredox dual catalysis provides a unique opportunity in organic synthesis, enabling the direct activation of C/Si/S–H bonds. However, the activation of O–H bonds of β,γ -unsaturated oximes poses a challenge due to their relatively high redox potential, which exceeds the oxidizing capacity of most currently developed photocatalysts. We here demonstrate that the combination of HAT and photoredox catalysis allows the activation of O–H bond of β,γ -unsaturated oximes. The strategy effectively addresses the oxime's high redox potential and offers a universal pathway for iminoxyl radical formation. Leveraging the versatility of this approach, a diverse array of valuable heterocycles have been synthesized with the use of different radical acceptors. Mechanistic studies confirm a HAT process for the O–H bond activation.

Received 22nd August 2023
Accepted 10th November 2023

DOI: 10.1039/d3sc04410f

rsc.li/chemical-science

1 Introduction

In the past few decades, the organic synthesis based on photoredox-catalyzed reactions was boosted by the exploitation of various visible-light-absorbing photocatalysts.¹ Hydrogen atom transfer (HAT) is a chemical step consisting of the concerted movement of a proton and an electron occurring between two substrates in a single kinetic step.² The incorporation of HAT catalysis and photoredox catalysis provides unique opportunities in organic transformations, and has emerged as a powerful tool for C/Si/S–H bond activation.³ In particular, when using quinuclidine as the HAT catalyst, after being oxidized by photocatalyst, the generated quinuclidinium radical cation is electrophilic, which could selectively abstract the more hydridic hydrogen atom of C/Si–H bond site according to the polarity-match between them, and regardless of the bond dissociation energies (BDEs) of C/Si–H.⁴ Oxygen radicals are widely used in both biological processes and organic synthesis.⁵ The generation of such radicals *via* direct cleavage of O–H bond is attractive but thermodynamically challenge,⁶ whereas the hydrogen of the O–H bond is protic, it is inaccessible to activate them through a polarity-match HAT pathway to give the oxygen radicals (Fig. 1a). Nevertheless, in addition to the polarity-match principle, the bond dissociation energies (BDEs) also

play an important role during the HAT process. β,γ -Unsaturated oximes are a type of useful building blocks that are used for the construction of isoxazoline molecules.⁷ The measurement of the redox potential value for β,γ -unsaturated oxime **1a** ($E_{p/2} = 2.2$ V vs. SCE in CH₃CN) indicates that it is relatively higher than that of most of the currently developed photocatalysts (See ESI Fig. S2†). This makes it challenging for the photocatalysts to directly oxidize the compound.⁸ As such, we conceived the possibility of activating the O–H bond in oxime **1a** through the use of 3-acetoxyquinuclidine as the HAT reagent. This is because the radical cation formed by 3-acetoxyquinuclidine has an H–N⁺ BDE (quinuclidine) of 100 kcal mol^{−1},⁹ which is higher than the O–H BDE of oxime (around 83 kcal mol^{−1}),¹⁰ enabling this process thermodynamically favored. If successful, this approach would resolve the challenge posed by the high redox potential of oxime in comparison to that of current photocatalysts, enabling the activation of the O–H bond and expanding the scope of C/Si–H bond activation to include the O–H bond, thus establishing a general pathway for the generation of the iminoxyl radical, as shown in Fig. 1b. Herein, we reported the first visible-light-mediated photoredox-catalyzed O–H bond activation of β,γ -unsaturated oximes by the merge of a thermodynamically favored HAT process, which provides a practical manner towards to a series of potential valuable isoxazoline molecules¹¹ (Fig. 1c).

2 Results and discussion

2.1. Optimization reaction conditions

Our investigation commenced with the visible-light-mediated oxyalkylation of the unactivated alkenes of β,γ -unsaturated

^aKAUST Catalysis Center (KCC), King Abdullah University of Science and Technology (KAUST), Thuwal 23955-6900, Saudi Arabia. E-mail: magnus.rueping@kaust.edu.sa

^bInstitute of Organic Chemistry, RWTH Aachen University, Landoltweg 1, D-52074 Aachen, Germany

† Electronic supplementary information (ESI) available. See DOI: <https://doi.org/10.1039/d3sc04410f>

a Activation of the C/Si-H bond via using quinuclidine and its derivatives as HAT reagent relaying on polarity match

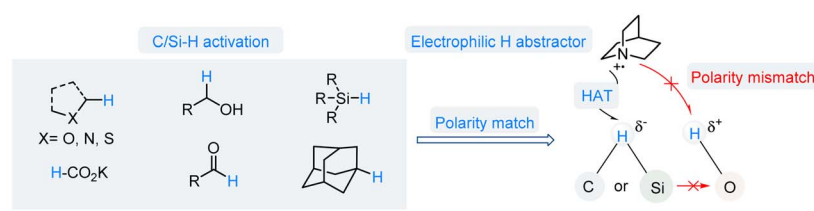
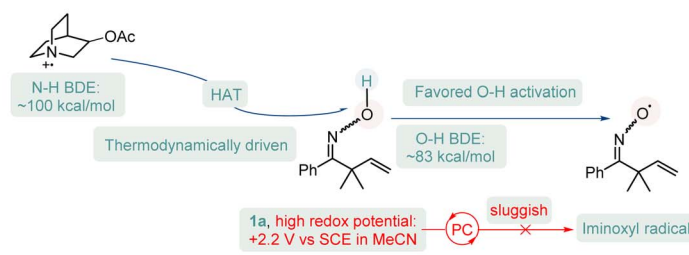
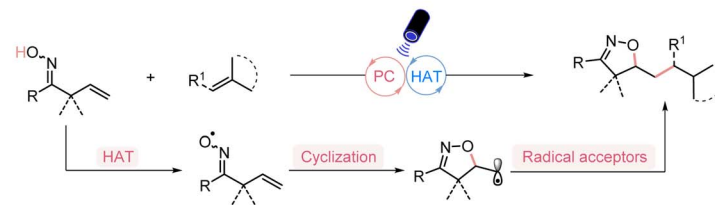
b Activation of the O-H bond of β,γ -unsaturated oxime via using 3-acetoxyquinuclidine as HAT reagent relaying on BDEs favored processc This work: oxyalkylation of β,γ -unsaturated oximes via HAT and photoredox dual catalysis

Fig. 1 Reaction design: the activation of O-H bond of β,γ -unsaturated oxime by HAT and photoredox dual catalysis.

oxime **1a** with but-3-en-2-one **2a**, under 34 W blue LED irradiation. After an exhaustive screening of various photocatalysts, solvents, and bases (see ESI Table S1†), as shown in Table 1, the use of 1.0 mol% Ir[dF(CF₃)ppy]₂(dtbbpy)PF₆ (**PC1**) and a catalytic amount of 3-acetoxyquinuclidine (20 mol%) in CH₃CN provided the desired product in 72% yield (entries 1–6).

While the reaction proceeded well without a base, the yield decreased slightly (entry 7), which is reasonable as the optimal base 2,6-lutidine might facilitate the regeneration of the HAT catalyst and the formation of the product *via* proton transfer. DABCO can in principle also act as a HAT catalyst. However, in the presence of a catalytic amount of DABCO, the product **3a** was produced in a lower yield (entry 8).

A significant yield reduction was observed in the absence of 3-acetoxyquinuclidine (entries 9–10). The control experiments demonstrated that light and the photocatalyst are essential for this reaction to occur (entries 11–12).

2.2. Substrate scope investigation

With the optimal conditions in hand, we started to explore the scope of the transformation. As presented in Fig. 2, a series of Michael acceptors, unsaturated ketones, esters or nitriles, reacted smoothly to give the desired products **3a–3g** in moderate to good yields. Substituents at the α -position of

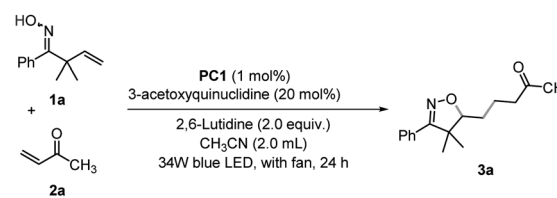
Michael acceptors (R^2 = Me and Ph) were also tolerated, and the corresponding products **3h–3k** were obtained with good yields.

The reaction of the β -substituted Michael acceptors also proceeded well without an apparent change in the yields **3l–3n**. Notably, the cyclic Michael acceptor **2o** also exhibited good reactivity. Besides Michael acceptors, styrene **2p** proved compatible with this reaction, yielding the desired product **3p** in moderate yield, even in the absence of a base. The scope of the reaction with respect to the β,γ -unsaturated oximes were also examined. Both electron-donating (4-MeC₆H₄, 4-MeOC₆H₄) and electron-withdrawing groups (4-ClC₆H₄, 4-BrC₆H₄ and 4-CNC₆H₄) were tolerated and gave the desired products **4a–4e** in 42–61% yields. Oximes bearing a meta-aryl substituent (3-ClC₆H₄ and 3-MeC₆H₄) or a meta/para-disubstitution (3,4-Cl₂C₆H₃ and 3,4-methylenedioxy) also exhibited good reactivity. The reaction of sterically hindered ortho-substituted (2-FC₆H₄) substrate also proceeded well. Notably, the oxime bearing a non-terminal olefin and 1-naphthyl group was also compatible, giving the corresponding product **4k** and **4l** in 46% and 52% yield, respectively. This compatibility was extended to heterocyclic substituents, resulting in the products **4m** and **4n** in 75% and 52% yields, respectively.

The *gem*-difluoroalkene moiety is viewed as a bioisostere of a carbonyl group and is of considerable interest for drug discovery. This is due to its electronic and steric effects, which



Table 1 Optimization for the oxyalkylation reaction



Reaction scheme showing the oxyalkylation of oxime **1a** with alkene **2a** to form product **3a**. Conditions: PC1 (1 mol%), 3-acetoxyquinuclidine (20 mol%), 2,6-lutidine (2.0 equiv.), CH₃CN (2.0 mL), 34W blue LED, with fan, 24 h.

Chemical structures of photocatalysts PC1, PC2, and PC3 are shown below the reaction scheme.

Entry	Variation from standard conditions ^a	Yield% ^b
1	None	72
2	PC2	30
3	PC3	Trace
4	DMF	7
5	DCE	39
6	DABCO	60
7	No base	64
8 ^c	DABCO	51
9	No 3-acetoxyquinuclidine, no base	8
10	No 3-acetoxyquinuclidine	19
11	No photocatalyst, no base	0
12	No blue light	0

^a Reaction conditions: β,γ -unsaturated oxime **1a** (0.4 mmol), but-3-en-2-one **2a** (0.2 mmol), photocatalyst (0.002 mmol), 2,6-lutidine (0.4 mmol), 3-acetoxyquinuclidine (0.04 mmol) in CH₃CN (2.0 mL) under irradiation of 34 W blue LED for 24 h with fan. ^b Isolated yield. ^c 0.04 mmol DABCO in the absence of 3-acetoxyquinuclidine and 2, 6-lutidine.

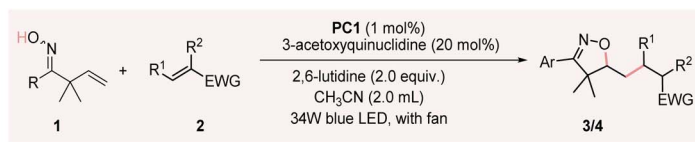
resemble those of corresponding aldehydes, ketones, and esters. It has been particularly applied to enhance metabolic stability.¹² In our continuing endeavor to expand the utility of this photoredox/HAT dual catalysis strategy, integrating the isoxazoline scaffold with the *gem*-difluoroalkene moiety presents a compelling avenue for drug discovery. With the same optimized reaction conditions applied, we were delighted to find that a variety of functionally substituted α -CF₃ alkenes were effectively applied as radical acceptors in the defluorinative *gem*-difluoroalkoxylation of β,γ -unsaturated oximes (Fig. 3). Different substitutions involving electron-donating groups (**6b–6e**, **6h–6j**) and weak electron-withdrawing groups (**6f** and **6g**) on the aryl ring of α -CF₃ styrenes do not significantly affect the reaction, resulting in desired products with moderate to good yields. It is worth noting that trifluoromethyl styrenes derived from ibuprofen (**5k**), gemfibrozil (**5l**) and oxaprozin (**5m**) reacted smoothly to give the difluorinated products. Moreover, thiophene substituted α -CF₃ styrene (**6n**) also underwent the expected reaction, giving the products with a 54% yield. In additions, we also investigated the scope of oxime moiety, with most oximes proceeding well under the optimized conditions.

Interestingly, while exploring the scope of α -CF₃ alkenes, we discovered that when α -CF₃ styrene bearing an electron-withdrawing group provides the CF₃-group containing product **7a–d** cyano (**7a**), acetyl (**7b**), and methyl ester (**7c**) with a good yield under standard conditions. For the proposed reaction mechanism, we propose the formation of an anion **Int. 7d'**, which rationalizes the formation of two distinct products. If **Int. 7d'** bears an electron-withdrawing group, it could render the carbon anion site more basic, favoring protonation over defluorination. In addition, the oxime moiety was also explored. A series of β,γ -unsaturated oximes participated in the process, giving the product **7e–7i** in good yields, regardless of the electronic property and position of the substituent on the aromatic ring. Notably, the thiophene substituted and α -dimethyl unsubstituted oximes also reacted well, providing the final products **7j–7l**.

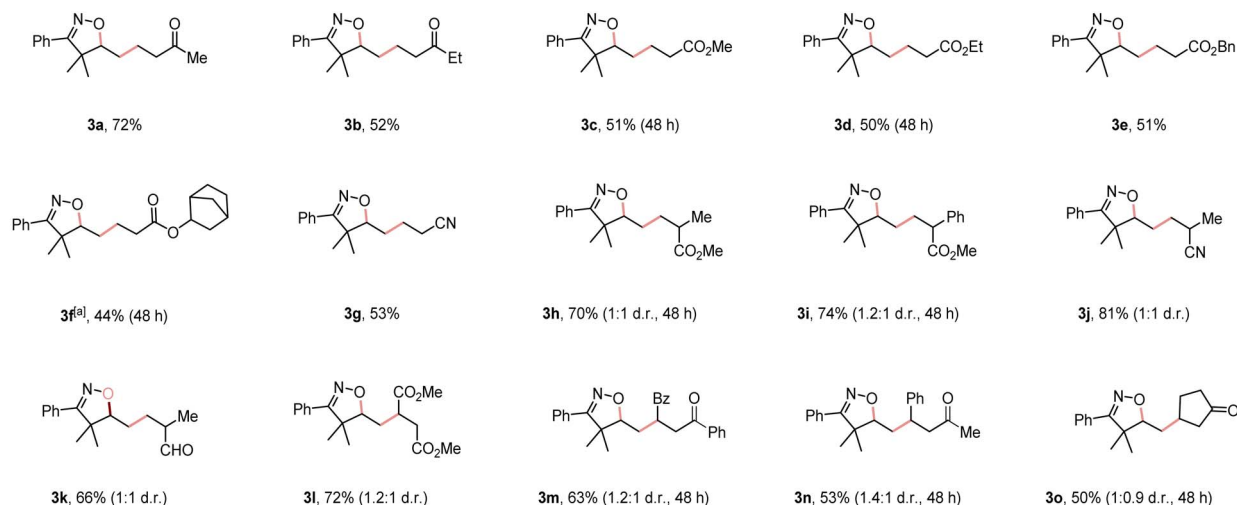
2.3. Scale-up reaction and mechanism studies

Given the broad applicability of our newly developed O–H bond activation and application in the synthesis of diverse isoxazolines, we performed a 20-fold scale-up without the use of a base and with a decreased 3-acetoxyquinuclidine loading (10 mol%); still providing an acceptable yield (Fig. 4a). To better understand the reaction mechanism, we performed several mechanistic studies to confirm the involvement of isoxazoline-containing alkyl radical in this reaction. Employing ethene-1,1-diylidibenzene as the radical acceptor under standard conditions and without a base yielded the radical-trapped product **8a** in 87% NMR yield (Fig. 4b). Moreover, when 3.0 equivalents of TEMPO (2,2,6,6-tetramethyl-1-piperidinyloxy) were added under standard conditions, formation of the desired product was completely inhibited. The TEMPO-trapped adduct **8b** was obtained instead (Fig. 4c). Two isotope-labeling studies further suggested the presence of carbon anion species in the catalytic cycle (Fig. 4d and e). To ascertain, that the iminoxyl radical was generated *via* a HAT mechanism rather than direct oxidation or a PT/ET pathway, comprehensive steady-state Stern–Volmer luminescence quenching experiments were performed (Refer to ESI Fig. S3–S17†). Specifically, to confirm the quenching of the excited photocatalyst **PC1*** by 3-acetoxyquinuclidine, various concentrations of 3-acetoxyquinuclidine were added to **PC1***. This yielded a linear fitting of the plots (Fig. 4f and g). The high redox potential value of **1a** pointed to a sluggish direct oxidation by **PC1***, as confirmed by the lack of observable luminescence quenching (Fig. 4h). To discern that **PC1*** could be quenched by oxime **1a** interacting with lutidine, quenching studies were performed with a mixture of oxime **1a** and varying concentrations of lutidine. However, no substantial quenching was observed (Fig. 4i), excluding the PT/ET pathway. Given that 3-acetoxyquinuclidine could possibly act as a base to abstract the proton from oxime or initiate a PCET (proton-coupled electron transfer) process, we conducted a quenching study between **PC1*** and a mixture of 3-acetoxyquinuclidine with different concentrations of oxime **1a**. However, varied concentrations of oxime **1a** did not impact the quenching rate, as the quenching rate of the mixture was





a. Scope of Michael acceptors



b. Scope of oximes

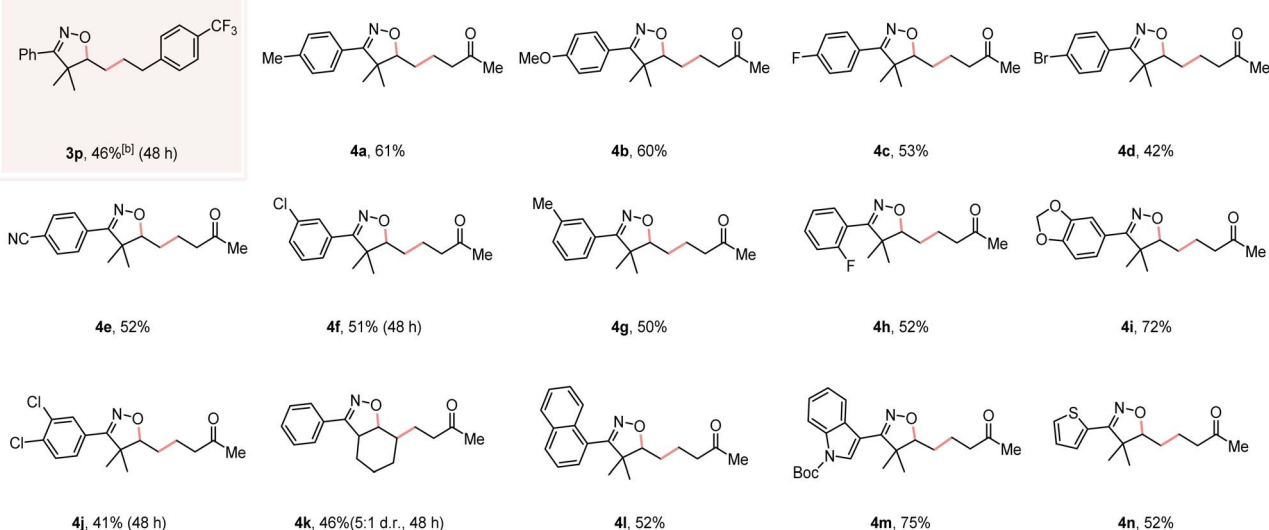


Fig. 2 Scope of different Michael acceptors and β,γ -unsaturated oximes. Reaction conditions: β,γ -unsaturated oxime **1** (0.4 mmol), Michael acceptors **2** (0.2 mmol), $\text{Ir}[\text{dF}(\text{CF}_3)\text{ppy}]_2(\text{dtbbpy})\text{PF}_6$ (0.002 mmol), 2,6-lutidine (0.4 mmol), 3-acetoxyquinuclidine (0.04 mmol) in CH_3CN (2.0 mL) at room temperature under irradiation of 34 W blue LED for 24 h or 48 h. The diastereomeric ratio of products are determined according to the ^1H NMR. ^[a] 0.2 mmol **1**, 0.4 mmol **2**. ^[b] Without 2,6-lutidine.

consistent with that of 3-acetoxyquinuclidine alone (Fig. 4j). Furthermore, to determine any potential interaction of oxime **1a** with 3-acetoxyquinuclidine and 2,6-lutidine, we conducted quenching studies using a mixture similar to the standard reaction concentrations. We found no significant quenching with this mixture, inferring that oxime **1a** does not interact with the other reaction components (Fig. 4k). In addition, we undertook cyclic voltammetry (CV) experiments involving oxime

1a and 2,6-lutidine (ESI, Fig. S2†). Our findings revealed that the presence of 2,6-lutidine appears to inhibit the oxidation of oxime **1a**. This observation prompted us to further explore the impact of 3-acetoxyquinuclidine on the redox potential of **1a**. Therefore, we conducted CV measurements on a mixture of oxime **1a** and 3-acetoxyquinuclidine. In comparison to the CV diagram of oxime **1a**, we noted distinct differences in the shape of the CV diagram for this mixture, particularly within the



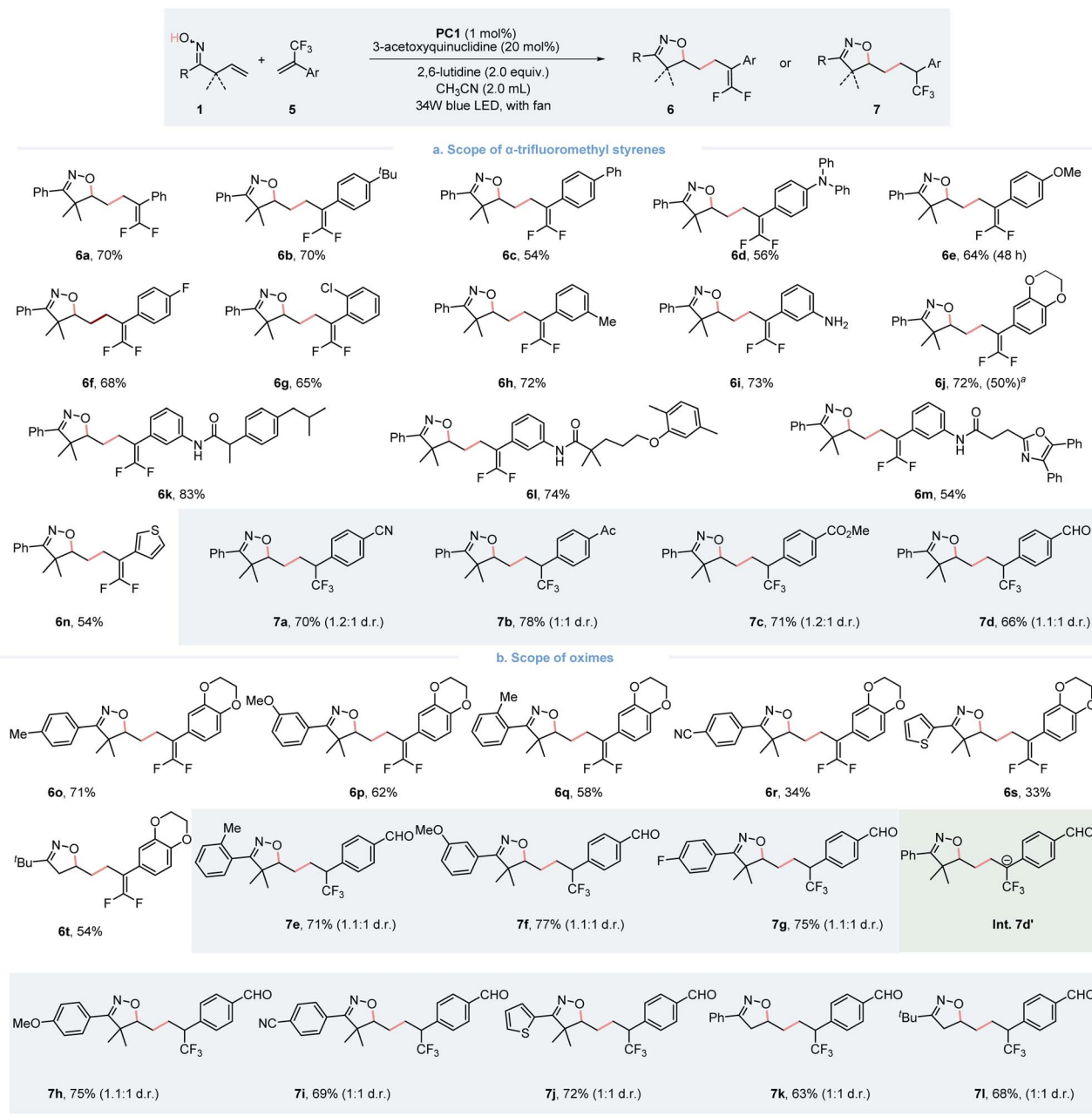


Fig. 3 Scope of different α -trifluoromethyl styrenes and β,γ -unsaturated oximes. Reaction conditions: β,γ -unsaturated oximes **1** (0.4 mmol), α -CF₃ styrenes **5** (0.2 mmol), Ir[dF(CF₃)ppy]₂(dtbbpy)PF₆ (0.002 mmol), 2,6-lutidine (0.4 mmol), 3-acetoxyquinuclidine (0.04 mmol) in CH₃CN (2.0 mL) under irradiation of 34 W blue LED for 24 h or 48 h with fan. The diastereomeric ratio of products **7** are determined according to the ¹H NMR. ^a Without 2,6-lutidine.

region corresponding to **1a**. This discrepancy arises from the overlap with a portion of the 3-acetoxyquinuclidine region in the diagram. Additionally, we conducted experiments involving oxime **1a** in conjunction with both, 3-acetoxyquinuclidine and 2,6-lutidine. Owing to the overlapping regions of these three components, we cannot make direct comparisons. However, despite this complication, 3-acetoxyquinuclidine exhibits the clear propensity for oxidation as the primary species in these mixtures. This can be attributed to the considerably lower redox potential within the system, as detailed in ESI Fig. S2.† These

results align with the outcomes of our Stern–Volmer quenching experiments which revealed that, in the presence of 2,6-lutidine and/or oxime **1a**, the quenching efficiency of 3-acetoxyquinuclidine towards photocatalyst **PC1** remained largely consistent.

2.4. DFT calculation and proposed mechanism

Furthermore, we conducted density functional theory (DFT) calculations (Fig. 5a) to further verify the HAT process. The 3-acetoxyquinuclidinyl radical cation (**V**), formed through



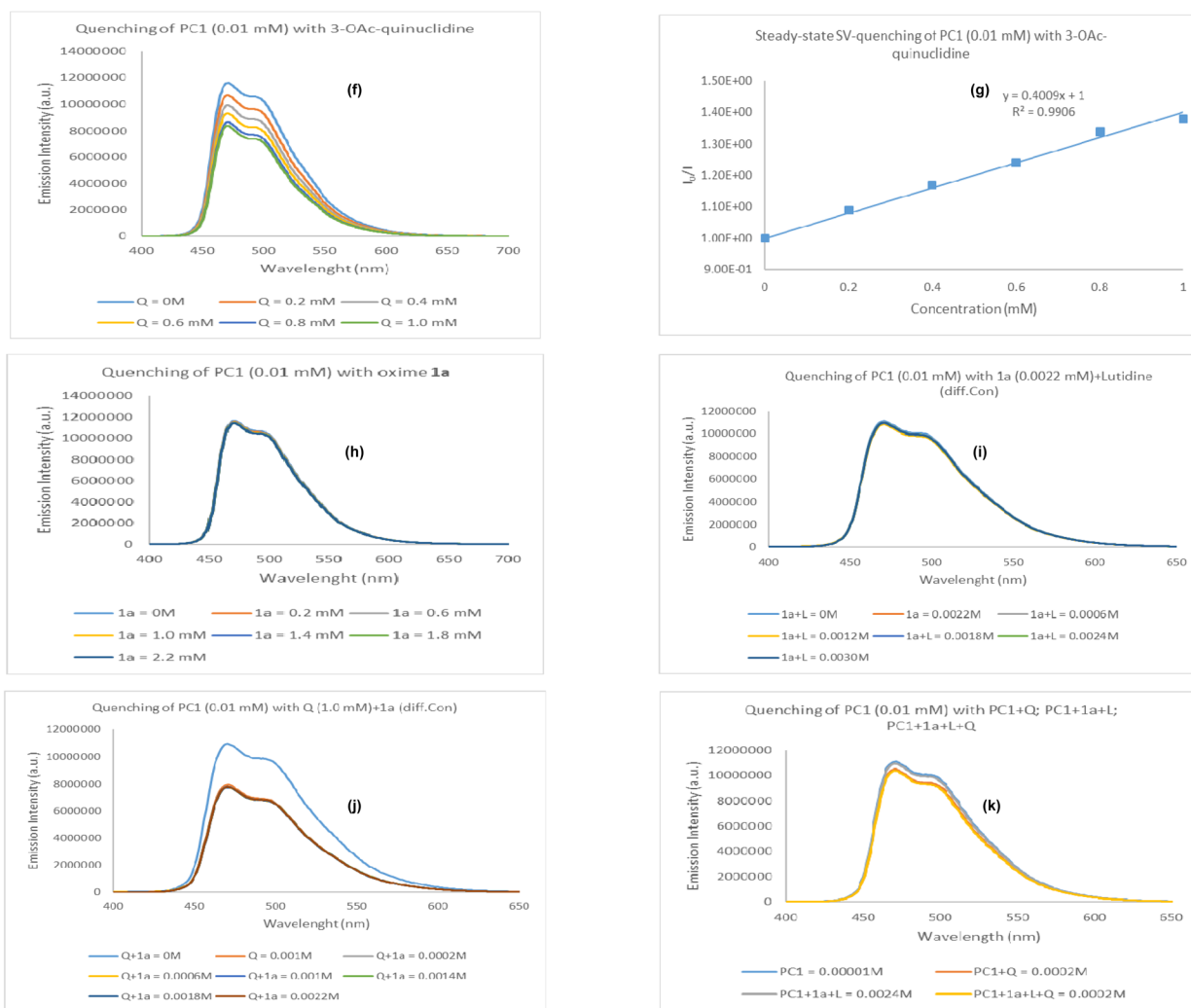
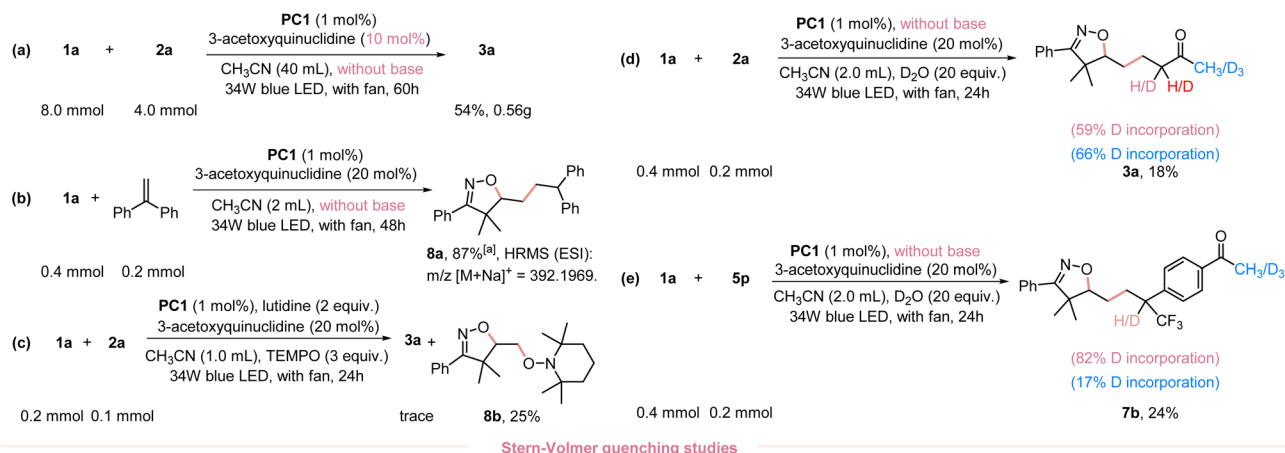


Fig. 4 (a) 20-fold scale-up reaction. (b) Isoxazoline-containing alkyl radical capture reaction by styrene. (c) Isoxazoline-containing alkyl radical capture reaction by TEMPO. (d) Isotope-labelling experiment of Michael acceptor (e) isotope-labelling experiment of α -CF₃ alkenes. (f–k) Stern–Volmer quenching experiments. ^[a] NMR yield using CH₂Br₂ as the internal standard.

oxidation by the excited $^*Ir^{III}$ photocatalyst, can abstract a hydrogen atom from oxime **1a** with an energy barrier of 18.9 kcal mol^{−1}. Following the HAT process, the generated

iminoxyl radical **VI** and amine cation **X** are 17.1 kcal mol^{−1} more stable. Thus, the HAT process is both kinetically feasible and thermodynamically favored. Subsequently, iminoxyl radical **VI**



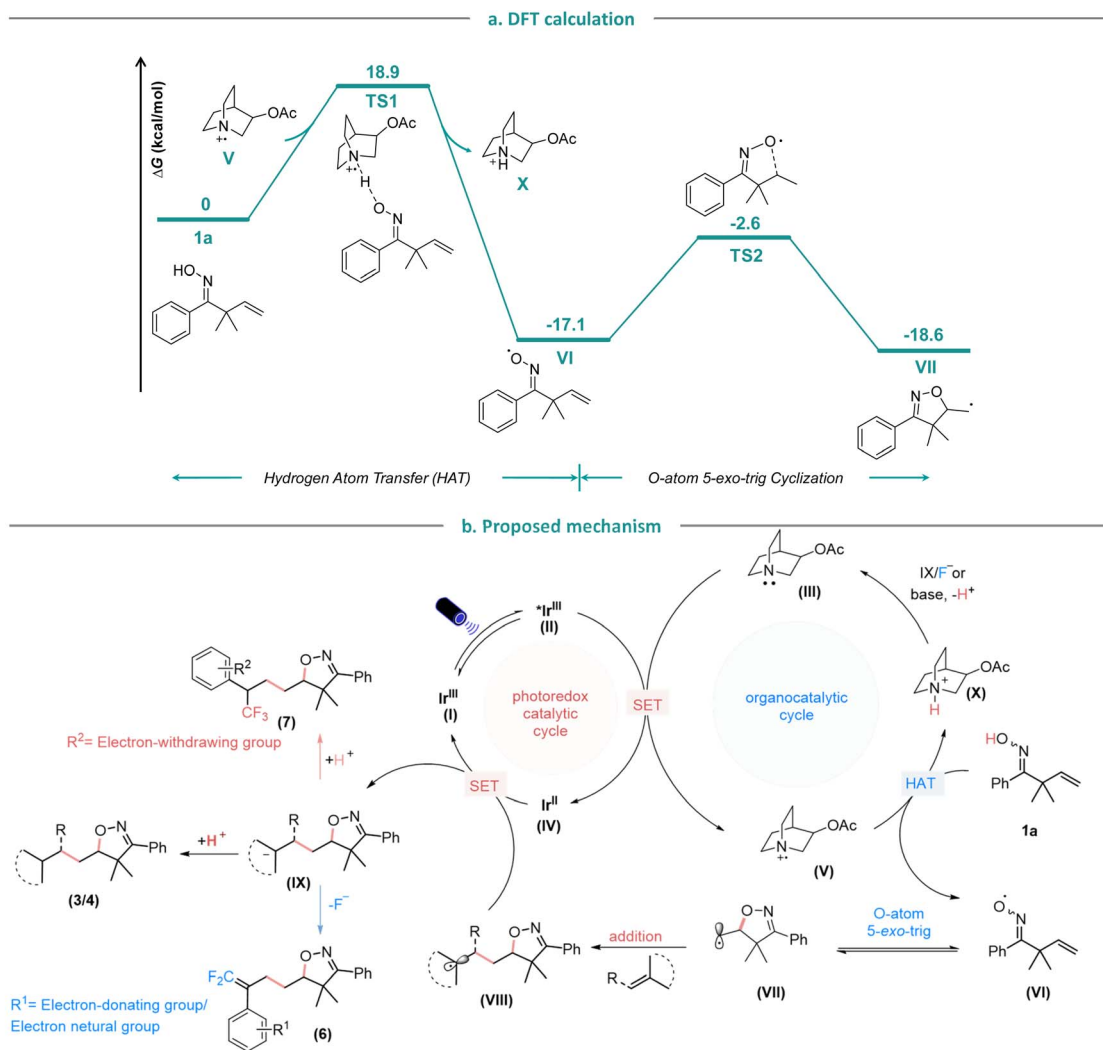


Fig. 5 (a). DFT calculation of hydrogen atom transfer and cyclization steps. (b). Proposed mechanism.

undergoes a 5-*exo-trig* cyclization with an energy barrier of 14.5 kcal mol⁻¹, leading to the formation of the C-centered isoxazoline alkyl radical **VII**. Based on the experimental and computational mechanistic studies, as well as prior research,^{3a,7j} a plausible mechanism for this photoredox-catalyzed HAT protocol is proposed (Fig. 5b).¹³ Firstly, the Ir^{III} complex (**I**) is irradiated by the visible light to give a long-lived triplet excited state *Ir^{III} oxidant (**II**), which is reduced in the presence of 3-acetoxyquinuclidine (**III**) to give Ir^{II} complex (**IV**) and amine radical cation (**V**). Then (**V**) abstracts the H-atom from β,γ -unsaturated oxime **1a** to form the iminoxyl radical (**VI**) which upon 5-*exo-trig* radical cyclization, yields the C-centered isoxazoline alkyl radical (**VII**), that subsequently adds to the radical acceptor to form the radical intermediate (**VIII**). Finally, the Ir^{II} complex (**IV**) is oxidized by (**VIII**) to regenerate the photocatalyst Ir^{III} complex (**I**) and the isoxazoline-containing carbon anion (**IX**). In the case of Michael acceptors, styrene and electron-withdrawing group substituted α -CF₃ alkenes (**IX**), abstracts a proton from amine cation (**X**) to regenerate HAT catalyst 3-acetoxyquinuclidine (**III**) to finish the catalytic cycle and to

provide the protonated products (**3/4/7**). Whereas the *gem*-difluoroalkene products (**6**) are obtained *via* defluorination when the α -CF₃ styrenes exhibits electron-donating or electron-neutral substituents. The main by-product in this reaction is the 5-methyl-4,5-dihydroisoxazole which could be formed by HAT of the carbon centered radical (**VII**) from **1a** to generate iminoxyl radical (**VI**).

3 Conclusions

In conclusion, we have developed the first visible-light-mediated photoredox and HAT dual catalyzed oxyalkylation of unactivated alkenes of β,γ -unsaturated oximes. This strategy produces a wide range of isoxazoline derivatives through reactions with different Michael acceptors, styrenes, or α -CF₃ alkenes. Our approach successfully addresses the high redox potential of the oxime, complements the activation of the O–H bond by quinuclidine, and provides a versatile pathway to generate iminoxyl radicals. Furthermore, this efficient and mild synthetic methodology has the potential to produce a diverse



array of valuable isoxazoline compounds, which may contribute to advancements in drug discovery efforts. Further studies may be directed towards the further exploration of photoredox HAT dual catalysis generated iminoxyl radicals in synthesis and reaction development.

Data availability

Experiment procedures, characterization of the new compounds, and Cartesian coordinates of DFT calculations are available in the ESI.†

Author contributions

L. Y. and M. R. conceived and designed the experiments. L. Y., T. J., Y. M., and Y. C. performed the experiments and analysed the data. C. Z. performed the DFT calculation. R. K. performed the Stern-Volmer quenching experiments. M. R. directed the project. All authors discussed the experimental results and commented on the manuscript.

Conflicts of interest

There are no conflicts to declare.

Acknowledgements

This publication is based upon work supported by the King Abdullah University of Science and Technology (KAUST) Office of Sponsored Research (OSR) under CRG award no. URF/1/5082 and URF/1/4701. L. Y. thanks the China Scholarship Council. C. Z. acknowledges the KAUST Supercomputing Laboratory for providing computational resources from the supercomputer Shaheen II. We thank Dr Jeremy Bau for quantum yield measurement.

Notes and references

- (a) M. H. Shaw, J. Twilton and D. W. C. MacMillan, *J. Org. Chem.*, 2016, **81**, 6898–6926; (b) J. Twilton, C. Le, P. Zhang, M. H. Shaw, R. W. Evans and D. W. C. MacMillan, *Nat. Rev. Chem.*, 2017, **1**, 0052; (c) N. A. Romero and D. A. Nicewicz, *Chem. Rev.*, 2016, **116**, 10075–10166; (d) J. A. Milligan, J. P. Phelan, S. O. Badir and G. A. Molander, *Angew. Chem., Int. Ed.*, 2019, **58**, 6152–6163; (e) Q. Q. Zhou, Y. Q. Zou, L. Q. Lu and W. J. Xiao, *Angew. Chem., Int. Ed.*, 2019, **58**, 1586–1604; (f) C. Zhu, H. Yue, L. Chu and M. Rueping, *Chem. Sci.*, 2020, **11**, 4051–4064; (g) C. Zhu, H. Yue, Ji. Jia and M. Rueping, *Angew. Chem., Int. Ed.*, 2021, **60**, 17810–17831; (h) L. Yi, T. Ji, K.-Q. Chen, X. Yu Chen and M. Rueping, *CCS Chem.*, 2022, **4**, 9–30; (i) J. Zhang and M. Rueping, *Chem. Soc. Rev.*, 2023, **52**, 4099–4120.
- J. K. J. T. Hynes, H.-H. Limbach and R. L. Schowen, *Hydrogen-Transfer Reactions*, Wiley-VCH, Weinheim, 2007.
- Examples: (a) D. Hager and D. W. C. MacMillan, *J. Am. Chem. Soc.*, 2014, **136**, 16986–16989; (b) K. Qvortrup, D. A. Rankic and D. W. C. MacMillan, *J. Am. Chem. Soc.*, 2014, **136**, 626–629; (c) M. H. Shaw, J. Twilton and D. W. C. MacMillan, *J. Org. Chem.*, 2016, **81**, 6898–6926; (d) Y.-Y. Gui, X.-W. Chen, W.-J. Zhou and D.-G. Yu, *Synlett*, 2017, **28**, 2581–2586; (e) Y.-Y. Gui, L.-L. Liao, L. Sun, Z. Zhang, J.-H. Ye, G. Shen, Z.-P. Lu, W.-J. Zhou and D.-G. Yu, *Chem. Commun.*, 2017, **53**, 1192–1195; (f) R. Zhou, Y. Y. Goh, H. Liu, H. Tao, L. Li and J. Wu, *Angew. Chem., Int. Ed.*, 2017, **56**, 16621–16625; (g) J. Twilton, M. Christensen, D. A. DiRocco, R. T. Ruck, I. W. Davies and D. W. C. MacMillan, *Angew. Chem., Int. Ed.*, 2018, **57**, 5369–5373; (h) J. Ye, I. Kalvet, F. Schoenebeck and T. Rovis, *Nat. Chem.*, 2018, **10**, 1037–1041; (i) V. Dimakos, H. Y. Su, G. E. Garrett and M. S. Taylor, *J. Am. Chem. Soc.*, 2019, **141**, 5149–5153; (j) H.-B. Yang, A. Feceu and D. B. Martin, *ACS Catal.*, 2019, **9**, 5708–5715; (k) J. Hou, A. Ee, H. Cao, H. W. Ong, J. H. Xu and J. Wu, *Angew. Chem., Int. Ed.*, 2018, **57**, 17220–17224; (l) M. Jouffroy, C. B. Kelly and G. A. Molander, *Org. Lett.*, 2016, **18**, 876–879; (m) E. L. Tyson, Z. L. Niemeyer and T. P. Yoon, *J. Org. Chem.*, 2014, **79**, 1427–1436; (n) L. Capaldo and D. Ravelli, *Eur. J. Org. Chem.*, 2017, **2017**, 2056–2071; (o) M. H. Shaw, V. W. Shurtleff, J. A. Terrett, J. D. Cuthbertson and D. W. MacMillan, *Science*, 2016, **352**, 1304–1308.
- W. Xiao, X. Wang, R. Liu and J. Wu, *Chin. Chem. Lett.*, 2021, **32**, 1847–1856.
- (a) P.-Z. Wang, J.-R. Chen and W.-J. Xiao, *J. Am. Chem. Soc.*, 2023, **145**, 17527–17550; (b) X. Wu, Z. Ma, T. Feng and C. Zhu, *Chem. Soc. Rev.*, 2021, **50**, 11577–11613; (c) A. Hu, J.-J. Guo, H. Pan and Z. Zuo, *Science*, 2018, **361**, 668–672; (d) Q. An, Y.-Y. Xing, R. Pu, M. Jia, Y. Chen, A. Hu, S.-Q. Zhang, N. Yu, J. Du and Y. Zhang, *J. Am. Chem. Soc.*, 2022, **145**, 359–376; (e) E. Tsui, H. Wang and R. R. Knowles, *Chem. Sci.*, 2020, **11**, 11124–11141; (f) L. Chang, Q. An, L. Duan, K. Feng and Z. Zuo, *Chem. Rev.*, 2021, **122**, 2429–2486.
- (a) J. Hartung, *Eur. J. Org. Chem.*, 2001, **2001**, 619–632; (b) M. H. V. Huynh and T. J. Meyer, *Chem. Rev.*, 2007, **107**, 5004–5064; (c) E. Tsui, A. J. Metrano, Y. Tsuchiya and R. R. Knowles, *Angew. Chem., Int. Ed.*, 2020, **59**, 11845–11849.
- (a) M. D. Mosher, A. L. Norman and K. A. Shurrush, *Tetrahedron Lett.*, 2009, **50**, 5647–5648; (b) M.-K. Zhu, J.-F. Zhao and T.-P. Loh, *J. Am. Chem. Soc.*, 2010, **132**, 6284–6285; (c) D. Jiang, J. Peng and Y. Chen, *Org. Lett.*, 2008, **10**, 1695–1698; (d) Y.-T. He, L.-H. Li, Y.-F. Yang, Y.-Q. Wang, J.-Y. Luo, X.-Y. Liu and Y.-M. Liang, *Chem. Commun.*, 2013, **49**, 5687–5689; (e) Q. Wei, J.-R. Chen, X.-Q. Hu, X.-C. Yang, B. Lu and W.-J. Xiao, *Org. Lett.*, 2015, **17**, 4464–4467; (f) F. Chen, F.-F. Zhu, M. Zhang, R.-H. Liu, W. Yu and B. Han, *Org. Lett.*, 2017, **19**, 3255–3258; (g) W. Zhang, Y. Su, K.-H. Wang, L. Wu, B. Chang, Y. Shi, D. Huang and Y. Hu, *Org. Lett.*, 2017, **19**, 376–379; (h) L. Zhu, G. Wang, Q. Guo, Z. Xu, D. Zhang and R. Wang, *Org. Lett.*, 2014, **16**, 5390–5393; (i) R.-H. Liu, D. Wei, B. Han and W. Yu, *ACS Catal.*, 2016, **6**, 6525–6530; (j) B. Han, X. L. Yang, R. Fang, W. Yu, C. Wang, X. Y. Duan and S. Liu, *Angew. Chem., Int. Ed.*, 2012, **51**, 8816–8820; (k) J.-Q. Chen, N. Liu, Q. Hu, J. Liu, J. Wu, Q. Cai and J. Wu,



- Org. Chem. Front.*, 2021, **8**, 5316–5321; (l) Z. Li, L. Qian, H. Chen and X. Xu, *Synlett*, 2022, **33**, 293–295; (m) X. Q. Hu, J. Chen, J. R. Chen, D. M. Yan and W. J. Xiao, *Chem. – Eur. J.*, 2016, **22**, 14141–14146; (n) X.-L. Yang, Y. Long, F. Chen and B. Han, *Org. Chem. Front.*, 2016, **3**, 184–189; (o) X.-X. Peng, Y.-J. Deng, X.-L. Yang, L. Zhang, W. Yu and B. Han, *Org. Lett.*, 2014, **16**, 4650–4653; (p) X.-L. Yang, F. Chen, N.-N. Zhou, W. Yu and B. Han, *Org. Lett.*, 2014, **16**, 6476–6479.
- 8 X.-Q. Hu, G. Feng, J.-R. Chen, D.-M. Yan, Q.-Q. Zhao, Q. Wei and W.-J. Xiao, *Org. Biomol. Chem.*, 2015, **13**, 3457–3461.
- 9 W.-Z. Liu and F. G. Bordwell, *J. Org. Chem.*, 1996, **61**, 4778–4783.
- 10 (a) D. A. Pratt, J. A. Blake, P. Mulder, J. C. Walton, H.-G. Korth and K. U. Ingold, *J. Am. Chem. Soc.*, 2004, **126**, 10667–10675; (b) S.-S. Chong, Y. Fu, L. Liu and Q.-X. Guo, *J. Phys. Chem. A*, 2007, **111**, 13112–13125.
- 11 (a) C.-B. Xue, J. Wityak, T. M. Sielecki, D. J. Pinto, D. G. Batt, G. A. Cain, M. Sworin, A. L. Rockwell, J. J. Roderick and S. Wang, *J. Med. Chem.*, 1997, **40**, 2064–2084; (b) S. Castellano, D. Kuck, M. Viviano, J. Yoo, F. López-Vallejo, P. Conti, L. Tamborini, A. Pinto, J. L. Medina-Franco and G. Sbardella, *J. Med. Chem.*, 2011, **54**, 7663–7677; (c) J.-F. Cheng, Y. Huang, R. Penuliar, M. Nishimoto, L. Liu, T. Arrhenius, G. Yang, E. O'leary, M. Barbosa and R. Barr, *J. Med. Chem.*, 2006, **49**, 4055–4058; (d) R. E. Olson, T. M. Sielecki, J. Wityak, D. J. Pinto, D. G. Batt, W. E. Frietze, J. Liu, A. E. Tobin, M. J. Orwat and S. V. Di Meo, *J. Med. Chem.*, 1999, **42**, 1178–1192; (e) P. K. Poutiainen, T. Oravilahti, M. Perakyla, J. J. Palvimo, J. A. Ihalainen, R. Laatikainen and J. T. Pulkkinen, *J. Med. Chem.*, 2012, **55**, 6316–6327; (f) P. K. Poutiainen, T. A. Venäläinen, M. Peräkylä, J. M. Matilainen, S. Väisänen, P. Honkakoski, R. Laatikainen and J. T. Pulkkinen, *Bioorg. Med. Chem.*, 2010, **18**, 3437–3447.
- 12 (a) N. A. Meanwell, *J. Med. Chem.*, 2011, **54**, 2529–2591; (b) G. Magueur, B. Crousse, M. Ourévitch, D. Bonnet-Delpon and J.-P. Bégué, *J. Fluorine Chem.*, 2006, **127**, 637–642; (c) P. M. Weintraub, A. K. Holland, C. A. Gates, W. R. Moore, R. J. Resvick, P. Bey and N. P. Peet, *Bioorg. Med. Chem.*, 2003, **11**, 427–431; (d) C. Leriche, X. He, C.-w. T. Chang and H.-w. Liu, *J. Am. Chem. Soc.*, 2003, **125**, 6348–6349; (e) Y. Pan, J. Qiu and R. B. Silverman, *J. Med. Chem.*, 2003, **46**, 5292–5293; (f) J.-M. Altenburger, G. Y. Lassalle, M. Matrougui, D. Galtier, J.-C. Jetha, Z. Bocskei, C. N. Berry, C. Lunven, J. Lorrain and J.-P. Herault, *Bioorg. Med. Chem.*, 2004, **12**, 1713–1730.
- 13 Selected articles on hydrogen atom transfer from our group: (a) L. Huang, M. Szewczyk, R. Kancherla, B. Maity, C. Zhu, L. Cavallo and M. Rueping, *Nat. Commun.*, 2023, **14**, 548; (b) C. Zhu, H. Chen, H. Yue and M. Rueping, *Nat. Synth.*, 2023, **2**, 1068–1081; (c) R. Kancherla, K. Muralirajan, B. Maity, S. Karuthedath, G. S. Kumar, F. Laquai, L. Cavallo and M. Rueping, *Nat. Commun.*, 2022, **13**, 2737; (d) R. Kancherla, K. Muralirajan, B. Maity, S. Karuthedath, G. S. Kumar, F. Laquai, L. Cavallo and M. Rueping, *Nat. Commun.*, 2022, **13**, 2737; (e) B. Maity, C. Zhu, M. Rueping and L. Cavallo, *ACS Catal.*, 2021, **11**, 13973–13982; (f) B. Maity, C. Zhu, H. Yue, L. Huang, M. Harb, Y. Minenkov, M. Rueping and L. Cavallo, *J. Am. Chem. Soc.*, 2020, **142**, 16942–16952; (g) A. Dewanji, P. E. Krach and M. Rueping, *Angew. Chem., Int. Ed.*, 2019, **58**, 3566–3570; (h) Y. Cai, Y. Tang, L. Fan, Q. Lefebvre, H. Hou and M. Rueping, *ACS Catal.*, 2018, **8**, 9471–9476; (i) L. Huang and M. Rueping, *Angew. Chem., Int. Ed.*, 2018, **57**, 10333–10337.

